Ab initio calculations of the atomic and electronic structure of diamond (111) surfaces with steps

G. Kern and J. Hafner

Institut für Theoretische Physik and Center for Computational Materials Science, Technische Universität Wien,
Wiedner Hauptstraße 8-10, A-1040 Wien, Austria
(Received 30 January 1998)

We present *ab initio* local-density-functional calculations of the atomic and electronic structure of stepped diamond (111) surfaces. The relaxation of an ideal monoatomic step with bulk-terminated terraces results in sp^2 bonding near the step. The spacing between the surface layers is also increased. A (2×1) reconstruction of the terraces lowers the surface energy and decreases the distance between the first two bilayers, but the step energy is increased. As on the flat (111) surface, hydrogen stabilizes the unreconstructed (1×1) surface on the terraces. The carbon atoms at the edge of the step have two dangling bonds. As the energy gained by forming an extra C-H bond is larger than the step-formation energy, exposure of C(111) to atomic hydrogen can lead to a roughening of the surface. The local electronic structure close to the step has been investigated. [S0163-1829(98)07128-8]

I. INTRODUCTION

Due to the technological importance of thin diamond films as wear-resistant surface coatings and as a promising material for high-temperature electronics, an enormous research effort has been directed towards a better understanding of their synthesis by chemical vapor deposition (CVD) techniques.[1] The first feature determining the growth rate of a diamond film in contact with a carbon-hydrogen plasma is the number of active diamond growth sites, i.e., surface carbon sp^3 radicals, which is determined by the equilibrium between the removal of H from C-H bonds at the surface and the recombination of gaseous hydrogen with the free surface C radicals. The second feature is the addition of the growth species to the surface radicals (under usual CVD conditions methyl radicals and acetylene are the most abundant species, but other C_nH_m radicals as well as atomic C may reach significant concentrations). A unique aspect of diamond growth is the competition between the deposition of sp^2- and sp^3-type carbons—in contrast to silicon where sp^2-hybridized species do not exist. For an understanding of these elementary reactions a detailed knowledge of the structural and electronic properties of clean and hydrogenated diamond surfaces is required. During the last decade, *ab initio* local-density calculations have lead to a thorough understanding of the properties of the low-index surfaces of diamond under various degrees of hydrogenation.[2–9]

Although most mechanisms for CVD growth have been described in terms of (111), (100), or (110) surfaces, a close inspection of these surfaces structures shows that there are only a few elementary sites that are favorable for hydrocarbon attachment.[10] Figure 1 shows that steps on (111) surfaces lead to the formation of small facets with a geometry identical to that of either the (110) or (100) surfaces. Such steps on diamond (111) surfaces are assumed to form the starting point for a growth sequence based on the addition of acetylene or methyl radicals.[11,12]

However, the model sketched in Fig. 1 assumes a bulk-terminated structure of both the (111) and (110) or (100) surfaces. It is now well established that the clean (111) and

(100) surfaces undergo a (2×1) reconstruction [which will be removed by a monolayer hydrogenation on the (111), but not on the (100) surface],[6,7] whereas the (110) surface does not reconstruct.[9] It is largely unknown how a possible reconstruction will affect the surface bond lengths and angles, the next-nearest-neighbor environment, and the relative sp^2/sp^3
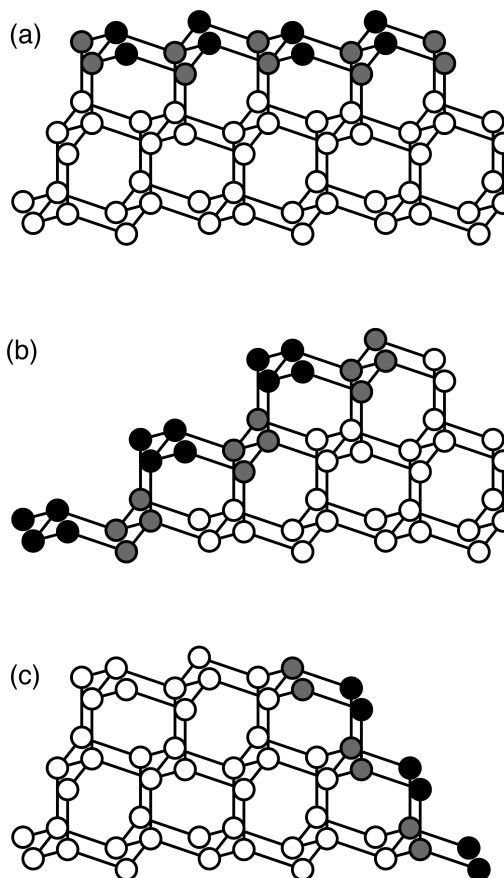

FIG. 1. Diagrams of the diamond (111) surface and steps. All circles represent carbon atoms. Black and gray circles illustrate the first and second layer of (a) a {111} plane, (b) a {110} plane, and (c) a {100} plane.

character of the C-C bonds close to steps under various degrees of hydrogenation. This is precisely the problem we address in this paper.

The investigation of the structure and energetics of steps on diamond surfaces has acquired additional interest by the observation that a roughening transition occurs on the Si(111) surface[13] and the prediction, based on Monte Carlo simulations, that roughening and preroughening transitions occur on the diamond (111) surface.[14] A conventional roughening transition is driven by a vanishing free energy of steps (ledge energy) on the surface and results in the spontaneous formation of steps eliminating the facet from the equilibrium crystal shape. A preroughening transition results in a surface that is macroscopically flat, but microscopically rough due to the formation of steps with long-range up-down order. This transformation occurs when the free energy of an isolated step vanishes, although the ''disordered flat'' surface with an up-down sequence of steps is still stabilized by step-step interactions. A preroughening transition could lead to a dramatic lowering of the barrier for both growth and etching processes. However, so far the reconstruction of the surface and its possible influence on the ledge energy have not yet been considered in the modeling of the (pre)roughening transition. Here our study could provide valuable information.

The clean flat diamond (111) one-dangling-bond surface is known to reconstruct in a (2×1) geometry with π-bonded chains in the first two bilayers.[15] The structural details of the reconstruction such as intrachain dimerization and/or buckling of the surface chain are still the subject of debate. Early semiempirical calculations[15−18] and the molecular-dynamics study of Iarlori et al.[3] favor dimerized chains, whereas most ab initio studies[2,4,7] find undimerized chains. All theoretical calculations predict a flat surface with no buckling. The observed optical transition at 2 eV as seen by electron-energy-loss spectroscopy[19] is attributed to the presence of a gap in the surface band structure. However, a (2×1) surface with undimerized and unbuckled chains is semimetallic.[7] Many-electron effects on the surface gap have been studied by Kress et al.[20] within the GW approximation. The conclusion is that the GW approach predicts a surface gap only if applied to a dimerized surface geometry, but not for symmetric or buckled chains. Huisman et al. performed an x-ray diffraction structure analysis[21] and a medium-energy ion scattering study[22] of the reconstructed diamond (111) (2×1) surface. They report a buckling of the surface chains by 0.3 Å and no dimerization.

Deposition of a monolayer of hydrogen leads to a dereconstruction of the surface. The structure of the (1×1):H surface is almost ideally bulk terminated and the electronic structure of the subsurface layers is nearly bulklike.[7] Annealing of the hydrogenated surface removes the hydrogen and the surface reconstructs in the (2×1) structure. Pate[23] showed that after subsequent anneals the low-energy electron diffraction (LEED) pattern remains (1×1), although the photoelectron spectra are the same as on a clean (2×1) surface. He related the persistence of the (1×1) LEED pattern to a roughening of the surface.

Scanning tunneling microscopy has been employed in the observations of CVD diamond (111) surfaces by Sasaki and Kawarada.[24] They report on H-terminated (1×1) surfaces with very straight single-atom height steps which form a downward slope in the (112) direction.

Davidson and Pickett[25] studied a stepped diamond (111) surface using a semiempirical tight-binding method. They claimed that the top bilayer of C atoms adjacent to the step spontaneously relaxes to a graphitic structure, which involves breaking the bonds to the second bilayer and reforming the sp^3 configuration into sp^2 bonding. However a reconstruction of the surface close to the step was not allowed.

This paper is organized as follows. In Sec. II we give a short outline of the theoretical and computational background. In Sec. III the computational aspects are listed. Section IV presents the results of the structural optimizations of the stepped surfaces. Their electronic properties are analyzed in Sec. V.

II. THEORY

For our calculations we used the Vienna *ab initio* simulation package,[26,27] which is based on the following principles.

(1) We use the finite-temperature version of local-density-functional (LDF) theory[28] developed by Mermin,[29] with the exchange-correlation functional given by Ceperley and Alder as parametrized by Perdew and Zunger.[30] Finite-temperature LDF theory introduces a smearing of the one-electron levels and helps to solve convergence problems arising from using a small set of **k** points for Brillouin-zone integrations, the use of fractional occupancies eliminates all instabilities that can arise from a crossing of levels in the vicinity of the Fermi energy. The variational quantity in finite-temperature LDF theory is the electronic free energy.

(2) The solution of the generalized Kohn-Sham equations is performed using an efficient matrix-diagonalization routine based on a sequential band-by-band residual minimization method (RMM) applied to the one-electron energies.[27,31]

(3) In the doubly iterative RMM method it is essential to use an efficient charge-density mixing-routine to avoid charge-sloshing problems. We use an improved Pulay mixing for calculating the new charge density and potential.[32] We have found that the sequential band-by-band algorithm combined with an efficient mixing algorithm is considerably faster than conjugate-gradient algorithms attempting a direct minimization of the energy by treating all bands simultaneously.[27]

(4) The optimization of the atomic geometry is performed via a conjugate-gradient minimization of the total energy with respect to the atomic coordinates.

(5) After moving the atoms, the new charge densities are estimated by extrapolating the results of the last steps.

(6) The calculation has been performed using fully non-local optimized ultrasoft pseudopotentials.[33,34] The nonlocal contributions are calculated in real space, using the optimized projectors introduced by King-Smith, Payne, and Lin.[35] Details of the pseudopotentials with a cutoff energy of $E_{cut} = 270$ eV are given in Refs. 7 and 36.

III. COMPUTATIONAL ASPECTS AND DEFINITIONS

A. Modeling of the surfaces

The stepped surface is modeled by slabs with periodic boundary conditions in all three directions with 120 C and 14 H atoms per unit cell [see Fig. 2(a)]. The triclinic cell con-
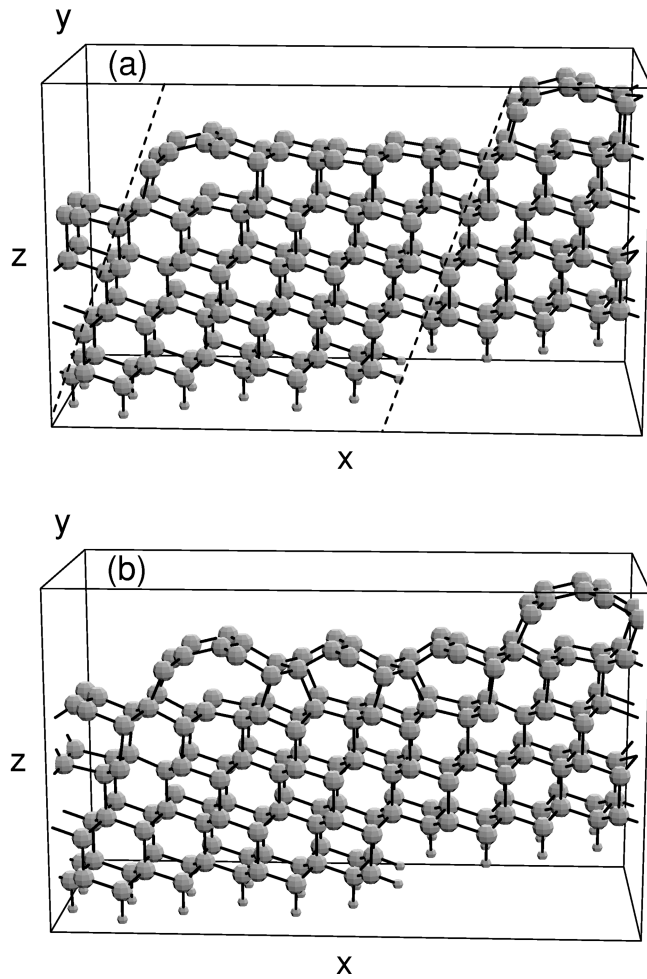
FIG. 2. Perspective views of the relaxed (a) and reconstructed (b) stepped C(111) surfaces. Carbon atoms, large spheres; hydrogen atoms, small spheres. The z axis is oriented along the [111] direction, the y axis along $[01\bar{1}]$, the x axis along $[2\bar{1}\bar{1}]$. The dashed line in (a) marks the extent of one supercell.

sists of 10 carbon layers separated by 6 Å of vacuum. The second surface is passivated with hydrogen to allow for a thinner slab. Only for calculating the absolute value of the energy of the ideal bulk-terminated step we had to use a symmetric slab. Therefore the accuracy of the absolute values of the energies is not as good as the relative energy differences between different configurations. In the $[2\ \bar{1}\ \bar{1}]$ (x) direction perpendicular to the steps we have six elementary units (sixfold rings) and in the $[0\ 1\ \bar{1}]$ (y) direction parallel to the step we have two unit cells, respectively, resulting in a (6×2) cell. Thus, the steps are separated by 13 surface C-C bond lengths. For the relaxation of the atoms, where we allowed the first four layers to relax, different starting configurations were used. Due to the symmetry of the forces the relaxation of the bulk-terminated step results in a structure where the terraces are in a (1×1) structure. In the following this structure is called *relaxed* step (or surface). As on the flat surface the reconstructed (2×1) surface is the stable structure, we also started the relaxation with (2×1) reconstructed terraces. This structure is called *reconstructed* step. Energetic, structural, and electronic details are given in the next sections.
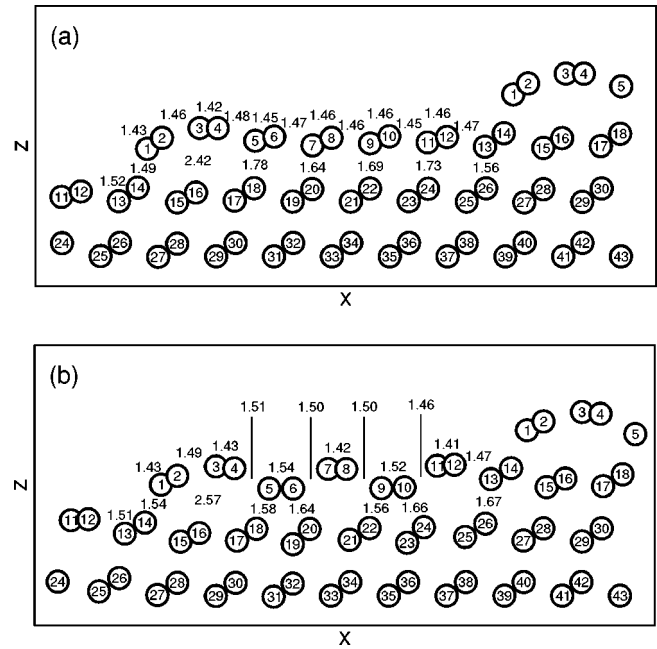

FIG. 3. Side view of the relaxed (a) and reconstructed (b) stepped C(111) surfaces. Interatomic distances are given in Å; the atom numbers are used for the discussion in the text and other figures.

In the bulk the interatomic distance is $d = 1.529$ Å at the calculated equilibrium lattice constant of $a_0 = 3.531$ Å. The experimental value of the lattice constant is $a_0 = 3.567$ Å. This difference is due to the characteristic LDF error. To introduce no stress we used the theoretical lattice constant for our surface calculations.

B. Definition of step energies

For the characterization of the steps we define two different energies. The ledge energy $E_{\text{ledge}} = (E_{\text{tot}} - E_{\text{bulk}} - N_{\text{surf}} E_{\text{flat}})/N_{\text{step}}$ is the energy of the step where E_{tot} is the total energy of the stepped surface, E_{bulk} is the total energy of a bulk crystal with the same number of atoms in the computational cell, N_{surf} is the number of surface atoms, E_{flat} is the surface energy per surface atom of a flat surface and N_{step} is the number of atoms at the edge of the step. Our (6×2) cell has 12 surface atoms and two step atoms, so $N_{\text{surf}} = 12$ and $N_{\text{step}} = 2$, respectively. For the different stepped surfaces the corresponding values of E_{flat} have to be taken, i.e., for instance, for the bulk-terminated step the surface energy of a flat bulk-terminated surface has to be used. The ledge energy is conventionally used to characterize the energy necessary to form a step on an otherwise flat surface. The second energy we call step energy and define it as $E_{\text{step}} = [E_{\text{tot}} - E_{\text{bulk}} - (N_{\text{surf}} - 2N_{\text{step}})E_{\text{flat}}]/N_{\text{step}}$. Thus it is the change in the energy of atoms located immediately at the step edge (in our case these are atoms 1 to 4, cf. Fig. 3 for the labeling of the atoms), because their surface energy is not subtracted in the calculation of the step energy. The rationale for the definition of this second energy is that the atoms 1 to 4 do not occupy positions corresponding to a (2×1) reconstructed or (1×1) relaxed terrace. Therefore, the subtraction of the surface energy for a flat (2×1) reconstructed surface for this atom does not describe the local changes at the step. The

TABLE I. Surface energies of the flat C(111) surfaces (in eV per surface site); calculated with a similar supercell and **k**-point settings ($\mathbf{k}_{1\times3\times1}$ corresponds to the $1\times3\times1$ grid and $\mathbf{k}_{2\times5\times1}$ to the $2\times5\times1$ grid, respectively) as the stepped surfaces (cf. text). E_{surf} refers to the absolute surface energy.

Structure	E_{surf} (eV/atom)	
	$\mathbf{k}_{1\times3\times1}$	$\mathbf{k}_{2\times5\times1}$
(1×1) ideal	2.683	2.714
(1×1) relaxed	2.130	2.153
(2×1)	1.328	1.375
(1×1):H	-2.778	-2.772

energies for the bulk and the flat surfaces were calculated with similar supercells and **k**-point settings as for the stepped surfaces (see Table I).

C. Brillouin-zone integration

For the Brillouin-zone integrations we used various grids of Monkhorst-Pack special points,[37] together with the Methfessel-Paxton technique for a smearing of the one-electron energies[38] within the finite-temperature LDF scheme. In the Methfessel-Paxton approach, the step function representing the Fermi-Dirac occupation probability is approximated by an expansion in terms of Hermite polynomials. In combination with a first-order approximation to the smearing function, a width of $\sigma=0.2$ eV has been determined as the optimal choice. For the calculation of the structural relaxation a $1\times3\times1$ grid with two irreducible **k** points in the Brillouin zone of our (6×2) cell seems to be sufficient, but for the structural details of the (2×1) reconstructed surface a denser $2\times5\times1$ grid with five irreducible **k** points is necessary (see discussion in Sec. IV). The surface energies and the local densities of state are also calculated with this denser $2\times5\times1$ grid to improve the resolution of the spectra.

IV. OPTIMIZATION OF THE SURFACE GEOMETRY

All energies of the stepped surfaces are compiled in Table II. We included also the energies calculated with the 1×3

$\times1$ **k**-point grid to show the convergence with respect to the **k**-point sampling. Except for the step energy of the reconstructed step all energies are converged within 1%. The reason for the larger error is that the step energy is very sensitive to the surface energy of the flat surface E_{flat}. For the flat C(111)-(2×1) surface the difference between the surface energies calculated with the two different **k**-point meshes is 0.05 eV per surface atom.

The step on the (111) surface can also be seen as a tiny (110) facet formed by atoms 1 and 2. So if we subtract the surface energy of one atom on the bulk-terminated diamond (111) surface [for atom 4, which is on the terrace of our (111) slab] from the step energy and divide this by 2 we get $E_{surf}=(6.70-2.71)/2=2.00$ eV. This is in good agreement with the surface energy of the bulk-terminated (110) surface of $E_{surf}=2.09$ eV.[9] The ledge energy of the bulk-terminated step is $E_{ledge}=1.27$ eV.

A. The hydrogenated step

The dangling bonds of the second surface were saturated by hydrogen. Twelve atoms saturate the dangling bonds in the [111] direction and two more saturate the extra dangling bonds on the step atoms 1 [there are two in our (6×2) cell]. For the structural optimization the hydrogen atoms and the first two layers of carbon atoms were allowed to relax until the forces were smaller than 0.1 eV/Å. Two carbon layers are enough because the relaxations on the fully hydrogenated diamond (111) and (110) surfaces are very small.[7–9] Also the residual forces in the first four layers of the hydrogenated surface are all smaller than 0.3 eV/Å; most of them are smaller than 0.15 eV/Å. All C-H bond lengths are 1.11 Å. On the step they are 0.005 Å shorter than on the flat part, the distance between the hydrogen atoms is 1.98 Å. The bond angle between the atom of the third layer, the step atom, and the hydrogen atom is 110°, i.e., close to the tetrahedral value of 109.5°.

The step energy of the hydrogenated is step $E_{step}=-8.13$ eV. If we again try to estimate the surface energy of the C(110)-(1×1):H facet we get $(-8.13+2.77)/2=-2.68$ eV, which is exactly the energy we got for the flat surface.[9] The reason for this perfect agreement is that the

TABLE II. Energetics of the stepped C(111) surfaces. E_{tot} refers to the energy of the stepped surface with 12 surface and 2 ledge atoms. ΔE_{tot} is the energy gain by relaxation or reconstruction, respectively, relative to the bulk-terminated surface. For E_{step} the surface energy of the flat surfaces with eight surface atoms was subtracted (see Table I), so it is the energy of the step atoms 1–4 (cf. Fig. 3 and text). E_{ledge} is the formation energy for a step (cf. text). The reference energy for the hydrogen atoms is the spin-polarized energy of a free hydrogen atom. The used **k**-point grid is indicated by $\mathbf{k}_{1\times3\times1}$ and $\mathbf{k}_{2\times5\times1}$, respectively.

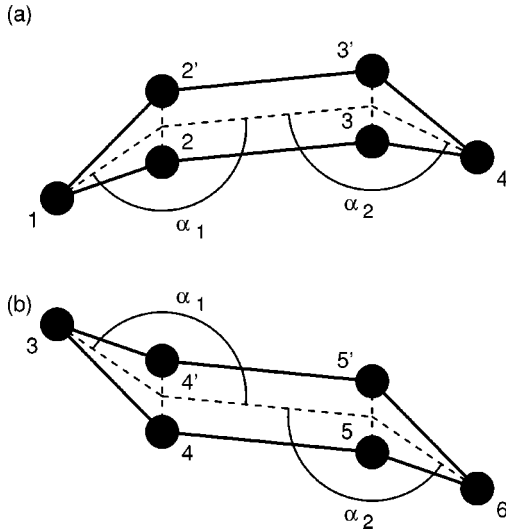| Structure		E_{tot} (eV/surface)	ΔE_{tot} (eV/surface)	E_{step} (eV/atoms 1-4)	E_{ledge} (eV/step atom)
Bulk terminated	$\mathbf{k}_{1\times3\times1}$	35.04		6.79	1.42
	$\mathbf{k}_{2\times5\times1}$	35.11		6.70	1.27
(1×1) relaxed	$\mathbf{k}_{1\times3\times1}$	26.43	-8.61	4.70	0.44
	$\mathbf{k}_{2\times5\times1}$	26.55	-8.57	4.66	0.36
(2×1) reconstructed	$\mathbf{k}_{1\times3\times1}$	21.55	-13.49	5.46	2.81
	$\mathbf{k}_{2\times5\times1}$	21.48	-13.63	5.24	2.49
(1×1):H relaxed	$\mathbf{k}_{1\times3\times1}$	-38.78	-73.82	-8.28	-2.72
	$\mathbf{k}_{2\times5\times1}$	-38.43	-73.55	-8.13	-2.58

FIG. 4. Sixfold rings at the surfaces: (a) boat configuration, (b) chair configuration. The dihedral angles α_1 and α_2 are indicated. The numbers correspond to the atom numbering of Fig. 3.

structural properties of the C(110)-(1×1):H surface and the hydrogenated step are very similar. The ledge energy is $E_{\text{ledge}}=-2.58$ eV. As we calculate the energies of hydrogenated surfaces always relative to the spin-polarized free hydrogen atoms, this means that if atomic hydrogen is present the formation of a step and the adsorption of the atomic hydrogen is an *exothermic* process. For the formation of a step in the presence of molecular H_2 we have to add the binding energy of the H_2 molecule to the ledge energy (the LDA value is 2.45 eV per H atom), resulting in an ledge energy of -0.13 eV. Thus if the hydrogenated (111) surface is exposed to atomic hydrogen, a creation of steps and therefore a roughening of the surface is energetically favorable, whereas with H_2 the energy gain of 0.13 eV is probably to low to overcome the energy barrier. Although we can give no estimation of the energy barrier, this confirms the experimentally observed roughening after the hydrogenation of the clean surface with atomic hydrogen.[23]

For the following calculations the hydrogen atoms and the carbon atoms of the second surface were kept fixed. All energy differences are calculated relative to this slab.

B. The clean relaxed step

Relaxing the slab in a constrained (1×1) geometry lowers the energy of the slab by $\Delta E_{\text{tot}}=-8.57$ eV. In connection with the surface energy of the flat relaxed (1×1) surface, this leads to a step energy of $E_{\text{step}}=4.66$ eV, which is 2.04 eV less than the step energy for a bulk-terminated geometry. The relaxation lowers also the ledge energy by 0.91 eV to $E_{\text{ledge}}=0.36$ eV.

The structure of the relaxed step is shown in Fig. 2(a); the bond lengths and the numbering of the atoms are displayed in Fig. 3(a). The first two zigzag rows next to the edge are relaxed outwards from the flat terrace. The bond length at the step is 1.43 Å. At the step the atoms 1-2-3-4-3′-2′ (primed numbers stand for equivalent sites displaced in the y direction) form twisted sixfold rings, so-called *boats* [see Fig. 4(a)], with bond lengths of 1.43 Å and 1.42 Å in the canted part [bonds 1-2(2′) and 3(3′)-4] and 1.46 Å in the flat part (bonds 2-3 and 3′-2′), respectively. The bond angles in the canted part are 122° between atoms 2-1-2′ and 124° between atoms 3-4-3′, respectively. The other bond angles are 117°. The dihedral angles are $\alpha_1=158.1°$ and $\alpha_2=165.1°$ [cf. Fig. 4(a)]. Next to the step the atoms 3-4-5-6-5′-4′ form *chairs* [see Fig. 4(b)] with $\alpha_1=161.6°$ and $\alpha_2=149.2°$ and bond angles of 123.1° between the atoms 4-3-4′, 119.5° between the atoms 5-6-5′ and between 115.6° and 116.9° on the other four triplets. The dihedral angles in the *chairlike* sixfold rings on the bulk-terminated flat (111) surface are 125.2°; the relaxation of the flat (1×1) surface increases the angle to 150.7°. The step energy characterizes the *boats*, although the step energy is the energy of atoms 1–4 but one *boat* consists of two atoms 2 and 3.

Davidson and Pickett[25] claimed that the relaxation of the C(111) step results in a graphitization of the surface with an average bond length of 1.44 Å in the surface plane and a layer spacing between the surface plane and the subsurface plane of 2.04 Å. Although we find that at the step the nearest-neighbor topology is similar to graphite due to the formation of the graphitic boat (graphite has a bond length of 1.42 Å, bond angles of 120°, and dihedral angles of 180°) and the large distance between atoms 3 and 16 of 2.42 Å [cf. Fig. 3(a)], the rest of the surface is similar to the flat C(111)-(1×1) surface. The average bond length of the flat part is 1.46 Å, which is the same as on the flat surface, and the average interlayer distance is 1.71 Å, which is again close to the value on the flat surface of 1.68 Å.

C. The clean reconstructed step

If the structural optimization is started from flat (2×1) reconstructed terraces, this leads to an energy gain of $\Delta E_{\text{tot}}=-13.63$ eV relative to the bulk-terminated surface. This is 5.06 eV lower than the total energy of the relaxed surface. Due to the much lower surface energy of the flat (2×1) surface, the step energy of the reconstructed surface is 5.24 eV, which is 0.58 eV higher than on the relaxed surface. The reason for that is that on the reconstructed surface the atoms 3 and 4 are further away from the step than on the (1×1) surface (see Fig. 3 for the bond lengths). The bond length between atoms 2 and 3 is increased to 1.49 Å and therefore the step on the (2×1) surface is under a larger strain, which costs energy. The dihedral angles of the boat on the reconstructed step are $\alpha_1=165.4°$ and $\alpha_2=160.6°$. Hence relative to the relaxed step the first angle is increased by 7° and the second is decreased by 5°. Due to the large rearrangements at the step relative to the (2×1) reconstructed chains the ledge energy is as high as 2.49 eV. This is 2.13 eV higher than on the relaxed step and even 1.22 eV higher than the ledge energy of the bulk-terminated step. On the reconstructed stepped surface the step energy characterizes the local bonding at the step better than the ledge energy, because the ledge energy assumes that atoms 2 and 4 are reconstructed, which is not the case. But if the terrace width on the stepped surface is larger than or equal to 4, the energy gain due to the reconstruction: $4[E_{\text{surf}}(2\times1)-\{E_{\text{surf}}(1\times1)\}]=4(2.15-1.37)=3.12$ eV] is larger than the energy loss at the step. So even with the minimal width of the terraces of four (then there are eight atoms in the first two layers—four
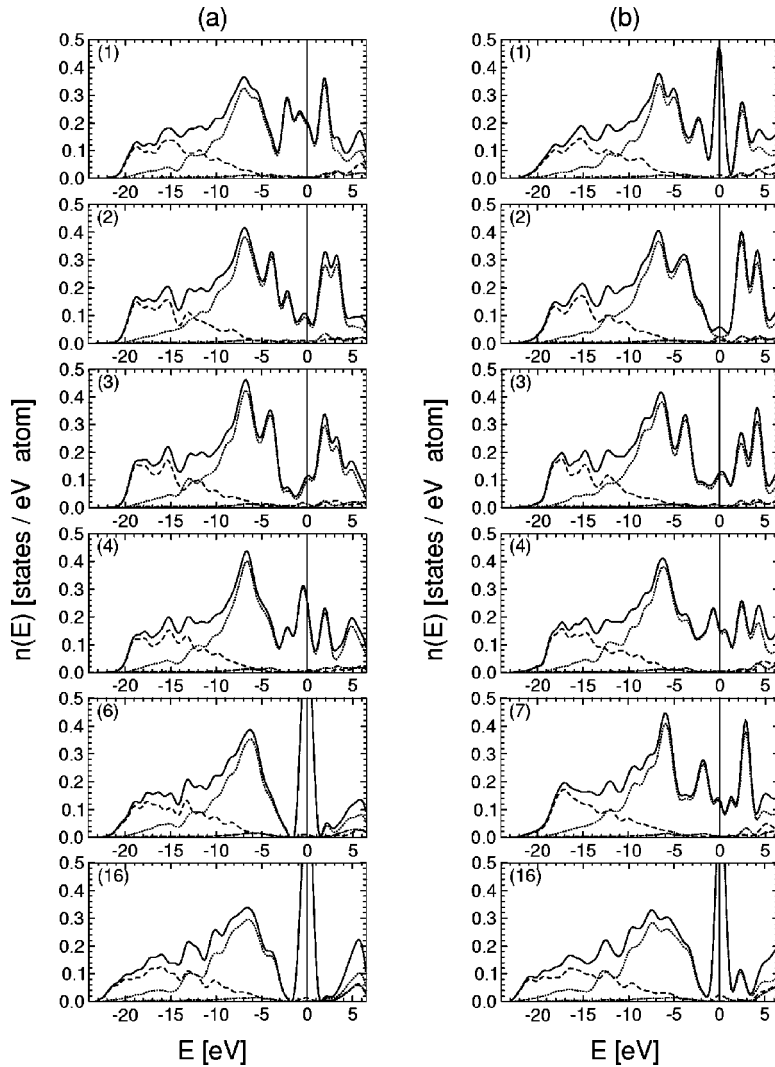
FIG. 5. Layer-resolved total and partial (angular-momentum decomposed) electronic density of states of the relaxed (a) and reconstructed (b) stepped C(111) surfaces. The numbers correspond to the numbering convention of Fig. 3. Full line, total DOS; dashed, dotted, and dash-dotted lines, s-, p-, and d-DOS, respectively. The energy is measured relative to the Fermi level.

of them are at the step and the other four are forming one fivefold and one sevenfold ring) the surface will reconstruct. This explains the experimental results of Pate:[23] on a rough surface there is no long-range order that would be needed to observe a (2×1) pattern, but the electronic structure is that of a clean reconstructed surface.

The interatomic distances of the reconstructed surface relaxed with the fine $2 \times 5 \times 1$ **k**-point grid are shown in Fig. 3(b). If we relax only with a $1 \times 3 \times 1$ **k**-point grid the step and the chains at the surface are dimerized, i.e., there is also a relaxation in the y direction. The dimerization varies between 1.2% at the step and 6.1% in the middle of the terrace. This dimerization is almost completely removed by the relaxation with the fine grid. Therefore to calculate the exact structural details of the reconstructed surface the number of **k** points is very crucial. Only a fully converged calculation can give the correct results. The **k**-point dependency is the same as on the flat surface.[7]

A difference between the flat and the stepped surfaces is the buckling along the chains. On the stepped surface it varies between 0.01 Å at the chain 7-8 and 0.04 Å at the chain 11-12 [see Fig. 3(b) for the numbering of the atoms]. The chain at the step (atoms 3-4) is buckled by 0.07 Å. This buckling is lower than the experimental result of 0.3 Å reported by Huisman et al.,[21,22] but higher than on the flat sur-

face. There is also a buckling between the chains of 0.15 Å. The buckling is not affected by the **k**-points sampling.

V. ELECTRONIC PROPERTIES

For the determination of the local density of states (LDOS) the eigenstates given in a plane-wave basis must be projected onto a local basis. This was done by projecting the individual plane-wave components onto the spherical waves within the atomic spheres drawn around each atomic site. The radius of the spheres is chosen such that the sum of the local density of states reproduces the total density of states (slightly larger than the Wigner-Seitz radius). Details of the projection technique are described in the paper by Eichler et al.[39] As the number of **k** points for the determination of the LDOS with the $2 \times 5 \times 1$ grid is not very high, we use a large Gaussian smearing of the eigenstates of 0.8 eV.

At the step (atoms 1 and 2) the density of states of the relaxed and the reconstructed surface (Fig. 5) are quite different. The LDOS of atom 1 of the relaxed (1×1) surface [see Fig. 5(a)] is very similar to that of the C(110) surface[9] (although on the flat surface we have used a much denser **k**-point grid), whereas on the reconstructed (2×1) surface the LDOS of atom 1 is sharply peaked at the Fermi level [see Fig. 5(b)]. This difference reflects the geometrical differ-
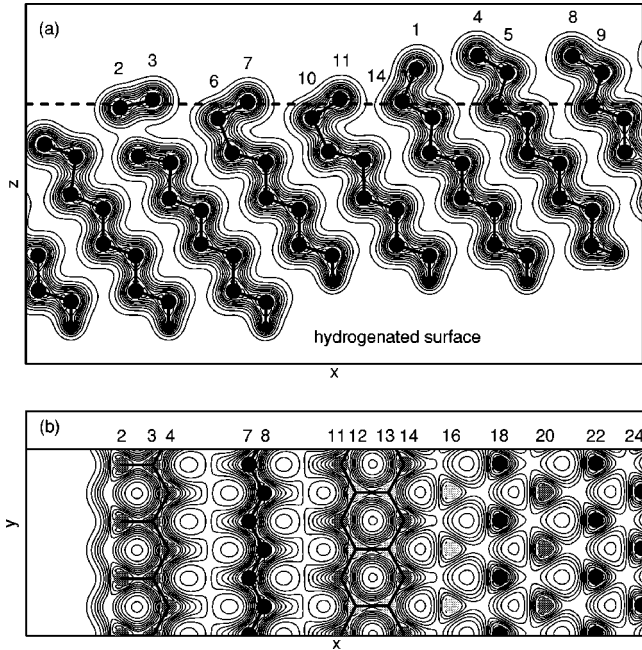
FIG. 6. Total charge density of the reconstructed stepped C(111) surface: (a) shown in a plane perpendicular to the surface, (b) shown in a plane parallel to the surface marked in (a) with the dashed line. The shading of the atoms corresponds to the distance of the atoms to the plane. Lighter shading means larger distance. The numbers of the atoms correspond to the numbering convention of Fig. 3. The contour intervals are 0.4 electrons per Å^3.

ences of the two surfaces. Atoms 3 and 4 of both surfaces are relatively similar in geometrical and electronic concerns.

On the terraces of the relaxed (1×1) and the reconstructed (2×1) surfaces (atoms 6 and 7, respectively) the LDOS are just like the corresponding ones on the flat surfaces. The atoms 16 on both surfaces have a high peak at the Fermi level. The reason is that these atoms have only three nearest neighbors and are therefore like the surface atoms of a flat (1×1) surface.

Figure 6 shows the total valence-charge distribution close to the step. The contour plot drawn in a plane perpendicular to the surface [Fig. 6(a)] displays very clearly the charge accumulation in chains of nearest-neighbor bonds in the bulklike regions, the reorientation of the surface-bonds at the flat terraces due to the (2×1) reconstruction, and the breaking of the nearest-neighbor bonds inside the edge of the step. A contour plot in a plane parallel to the surface [Fig. 6(b)] shows the bond charges associated with the π-bonded Pandey chains on the flat part of the terraces (atoms 7-8), distributions associated with the boat at the upper level of the step (atoms 1-2-3-4-3'-2'), and with the flattened chair at the lower edge of the step (atoms 11 to 14).

Electronic surface states associated with the step are analyzed in Figs. 7–9. Figure 7 shows the charge densities of several eigenstates with dangling-bond character distributed around the Fermi level. Part (a) shows the p_z-like dangling bonds belonging to atom 1 and 4, which are part of the graphitic boat at the upper edge of the step. These states are not too different from the dangling-bond states localized on the flat part of the terraces [atoms 7 and 11, see part (b)]. Similar dangling-bond states at essentially the same energy have also been identified on the flat reconstructed C(111)-
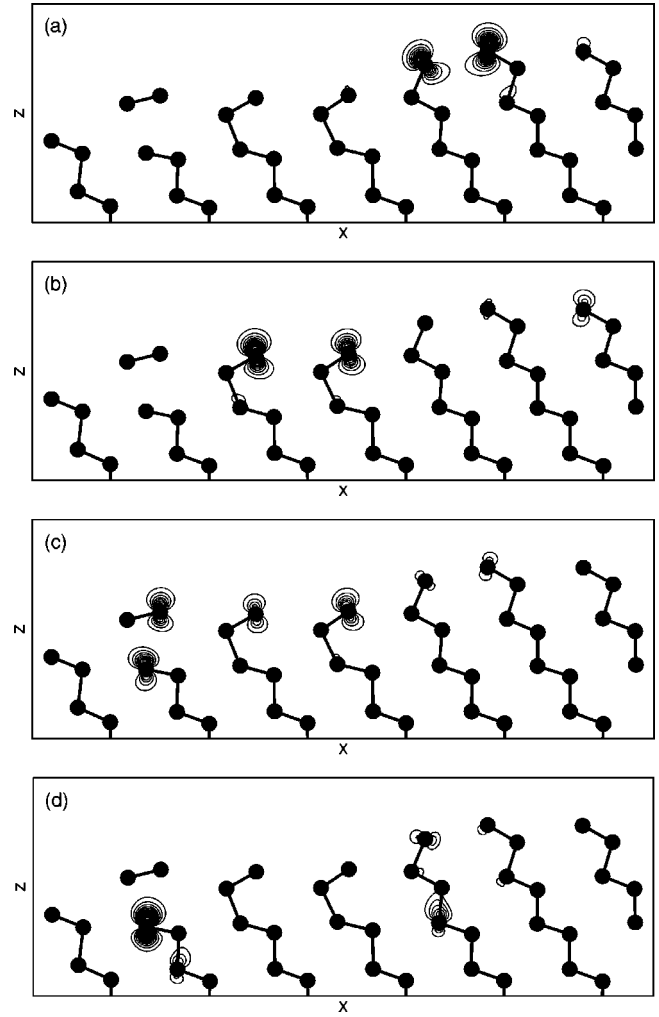

FIG. 7. Charge densities of the surface states in a plane perpendicular to the surface on the reconstructed stepped C(111) surface at Γ and (a) $E = -0.70$ eV, (b) $E = -0.33$ eV, (c) $E = -0.09$ eV, (d) $E = 0.24$ eV. The contour intervals are 0.04 electrons per Å^3 (cf. Fig. 6).

(2×1) surface.[7] Immediately at and slightly above the Fermi energy we find states with a strong dangling-bond character *inside* the step, located on the threefold-coordinated atom 16 [see Figs. 7(c) and (d)].

Figure 8 shows bonding (a) and antibonding (b) $pp\pi$ states localized on the graphitic boat (atoms 2 and 3). These states are similar to the $pp\pi$-surface states on the (110) surface located within the bulk gap. However, at the step edge the bonding-antibonding splitting is now much larger, placing the bonding and antibonding surface states close to the LDOS peaks at -3.5 eV and $+2.0$ eV. States contributing to the Pandey chains on the reconstructed terraces are also shown in Fig. 9 in a plane parallel to the surface. These states fall close to the p-like maximum of the bulk DOS and show therefore a strong coupling to bulk states.

VI. DISCUSSION AND CONCLUSIONS

We have performed *ab initio* local-density-functional investigations of the formation of steps on clean and hydrogenated C(111) surfaces. Our results show that as for the flat C(111) surface the atomic structure is dominated by a (2
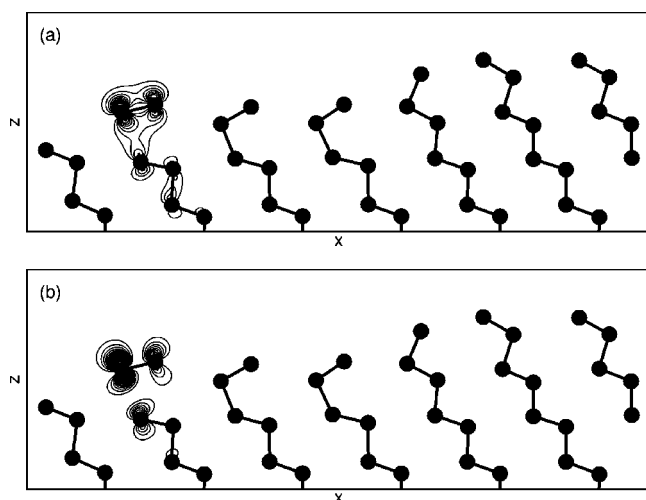
FIG. 8. Charge densities of the surface states in a plane perpendicular to the surface on the reconstructed stepped C(111) surface at Γ and (a) $E = -3.38$ eV, (b) $E = 1.74$ eV. The contour intervals are 0.04 electrons per Å^3 (cf. Fig. 6).
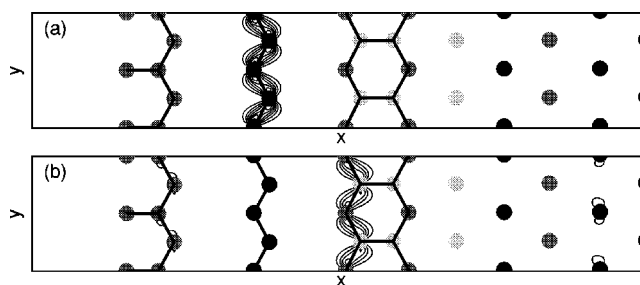

FIG. 9. Charge densities of the surface states in a plane parallel to the surface on the reconstructed stepped C(111) surface at Γ and (a) $E = -5.67$ eV, (b) $E = -5.92$ eV. The contour intervals are 0.04 electrons per Å^3 (cf. Fig. 6).

$\times 1$) reconstruction of the flat terraces on both sides of the step edge as long as the terraces extend over at least two zigzag rows of surface atoms running parallel to the step (a terrace width of four interatomic distances). In this case the gain in surface energy due to reconstruction overcompensates the higher energetic cost for step formation on the reconstructed surface. For a higher step density, however, a relaxed (1×1) geometry of the surface is stabilized. Close to the step edge, the bonding between the topmost bilayers is broken and the atoms in the upper bilayer assume a more graphitic arrangement. Our result that graphitization is restricted to the immediate environment of the step is in contradiction to the prediction of Davidson and Pickett (based on tight-binding calculations) (Ref. 25) that the step formation will induce a complete graphitization of the C(111) surface.

Hydrogenation stabilizes again a (1×1) geometry of the surface. At the upper edge of the step the C atom in the second layer has also a dangling bonds. Due to the adsorption of an extra H atom for this C-ledge atom, step formation is now an exothermic process. The ledge energy of -2.58 eV is now higher than the binding energy of hydrogen in the

H_2 molecule (2.45 eV/H atom). Hence, even the dissociative adsorption of H_2 on a flat C(111)-(2×1) surface could in principle induce a roughening of the surfaces. However, as demonstrated in Ref. 7, H adsorption initially leads to the formation of a metastable (2×1):H surface. Dereconstruction to the stable (1×1):H surface is associated with a barrier of about 2 eV per atom and hence will occur only if the surface is exposed to atomic hydrogen. Further hydrogen adsorption is an exothermic process since the energy gained by forming an extra C-H bond at the edge is higher than the step-formation energy. However, only on adsorption of atomic hydrogen will the energy difference be high enough to overcome an eventual barrier (not calculated). Therefore, only atomic H will induce step formation on the C(111) surface as observed by Pate.[23]

The electronic structure of the stepped surface has been studied in detail. We find that the existence of a step induces extra intensity in the bulk gap arising from dangling bond states localized at the edge atoms and immediately below the graphitic part of the upper terrace.

Whether the graphitization observed at the step-edge will also facilitate a temperature-induced graphitization of the entire C(111) surface is now the subject of intense *ab initio* molecular dynamics studies.[40] The calculated step geometries will also be useful for a more detailed analysis of models for CVD growth.

ACKNOWLEDGMENT

[1] *Synthetic Diamond: Emerging CVD Science and Technology*, edited by K. E. Spear and J. O. Carlsson (Wiley, New York, 1994).

[2] D. Vanderbilt and S. G. Louie, J. Vac. Sci. Technol. B **1**, 723 (1983); Phys. Rev. B **30**, 6118 (1984).

[3] S. Iarlori, G. Galli, F. Gygi, M. Parrinello, and E. Tosatti, Phys. Rev. Lett. **69**, 2947 (1992).

[4] A. Scholze, W. G. Schmidt, and F. Bechstedt, Phys. Rev. B **53**, 13 725 (1996).

[5] J. Furthmüller, J. Hafner, and G. Kresse, Europhys. Lett. **28**, 659 (1994).

[6] J. Furthmüller, J. Hafner, and G. Kresse, Phys. Rev. B **53**, 7334 (1996), and references cited therein.

[7] G. Kern, J. Hafner, and G. Kresse, Surf. Sci. **366**, 445 (1996).

[8] G. Kern, J. Hafner, and G. Kresse, Surf. Sci. **366**, 464 (1996).

[9] G. Kern and J. Hafner, Phys. Rev. B **56**, 4203 (1997).

[10] K. E. Spear and M. Frenklach, Pure Appl. Chem. **66**, 1773 (1994).

[11] M. Frenklach and K. E. Spear, J. Mater. Res. **3**, 133 (1988).

[12] D. N. Belton and S. J. Harris, J. Chem. Phys. **96**, 2371 (1992).

[13] D. Y. Noh, K. I. Blum, M. J. Ramstad, and R. J. Birgeneau, Phys. Rev. B **48**, 1612 (1993).

[14] D. L. Woodraska and J. A. Jaszczak, Phys. Rev. Lett. **78**, 258 (1997).

[15] K. C. Pandey, Phys. Rev. B **25**, 4338 (1982).

[16] D. J. Chadi, Phys. Rev. B **26**, 4762 (1982).

[17] R. Dovesi, C. Pisani, C. Roetti, and J. M. Ricart, Surf. Sci. **185**, 120 (1987).

[18] X. M. Zheng and P. V. Smith, Surf. Sci. **253**, 395 (1991).

[19] S. V. Pepper, Surf. Sci. **123**, 47 (1982).

[20] C. Kress, M. Fiedler, and F. Bechstedt, Europhys. Lett. **28**, 433 (1994).

[21] W. J. Huisman, M. Lohmeier, H. A. van der Vegt, J. F. Peters, S. A. de Vries, E. Vlieg, V. H. Etgens, T. E. Derry, and J. F. van der Veen, Surf. Sci. (to be published).

[22] W. J. Huisman, J. F. Peters, and J. F. van der Veen, Surf. Sci. (to be published).

[23] B. B. Pate, Surf. Sci. **165**, 83 (1986).

[24] H. Sasaki and H. Kawarada, Jpn. J. Appl. Phys., Part 2 **32**, L1771 (1993).

[25] B. N. Davidson and W. E. Pickett, Phys. Rev. B **49**, 14 770 (1994).

[26] G. Kresse and J. Hafner, Phys. Rev. B **47**, 558 (1993); **49**, 14 251 (1994).

[27] G. Kresse and J. Furthmüller, Comput. Mater. Sci. **6**, 15 (1996).

[28] W. Kohn and L. J. Sham, Phys. Rev. **140**, A1133 (1965).

[29] N. D. Mermin, Phys. Rev. **140**, A1141 (1965).

[30] J. P. Perdew and A. Zunger, Phys. Rev. B **23**, 5048 (1981).

[31] D. M. Wood and A. Zunger, J. Phys. A **18**, 1343 (1985).

[32] P. Pulay, Chem. Phys. Lett. **73**, 393 (1980).

[33] D. Vanderbilt, Phys. Rev. B **41**, 7892 (1990).

[34] G. Kresse and J. Hafner, J. Phys.: Condens. Matter **6**, 8245 (1994).

[35] R. D. King-Smith, M. C. Payne, and J. S. Lin, Phys. Rev. B **44**, 13 063 (1991).

[36] J. Furthmüller, J. Hafner, and G. Kresse, Phys. Rev. B **50**, 15 606 (1994).

[37] H. J. Monkhorst and J. D. Pack, Phys. Rev. B **13**, 5188 (1976).

[38] M. Methfessel and A. T. Paxton, Phys. Rev. B **40**, 3616 (1989).

[39] A. Eichler, J. Hafner, J. Furthmüller, and G. Kresse, Surf. Sci. **346**, 300 (1996).

[40] G. Kern and J. Hafner, Phys. Rev. B (to be published).